

# Influence of Confinement on Nominal Capacity and Curvature Ductility of Spun Piles

Putu Ogi Suryadinata, Tavio\*, I Gusti Putu Raka

Department of Civil Engineering, Institut Teknologi Sepuluh Nopember (ITS), Surabaya, Indonesia

Received January 27, 2023; Revised February 25, 2023; Accepted April 7, 2023

## Cite This Paper in the Following Citation Styles

(a): [1] Putu Ogi Suryadinata, Tavio, I Gusti Putu Raka, "Influence of Confinement on Nominal Capacity and Curvature Ductility of Spun Piles," *Civil Engineering and Architecture*, Vol. 11, No. 4, pp. 2255 - 2262, 2023. DOI: 10.13189/cea.2023.110442.

(b): Putu Ogi Suryadinata, Tavio, I Gusti Putu Raka (2023). *Influence of Confinement on Nominal Capacity and Curvature Ductility of Spun Piles*. *Civil Engineering and Architecture*, 11(4), 2255 - 2262. DOI: 10.13189/cea.2023.110442.

Copyright©2023 by authors, all rights reserved. Authors agree that this article remains permanently open access under the terms of the Creative Commons Attribution License 4.0 International License

**Abstract** Axial force-bending moment (P-M) interaction diagrams are indispensable in the design of spun piles. From the interaction diagrams, the capacity of the section to resist axial force and bending moment can be obtained based on the results of a cross-sectional analysis of strain and stress distributions. The construction of an interaction diagram generally requires manual neutral axis trial and error calculations, which are time-consuming. Hence, a time-saving and more accurate auxiliary program was developed using MATLAB. Confinement can change the shape of concrete stress-strain curves, as seen from increasing compressive stress in the cross-section at certain ultimate strains. Accounting for the effect of confinement will increase the ultimate strains, leading to a more ductile structure. The confinement models used include Mander et al., El-Dash and Ahmad, and Kusuma and Tavio. The variations included the effect of prestressing force, spiral spacing, and the impact of confinement reinforcement area. The results of the confinement variables affect the cross-sectional curvature ductility. If the spiral spacing is closer or the area of reinforcing bars is increased, the curvature ductility increases.

**Keywords** Curvature, Disaster Risk Reduction, Ductility, Spiral, Spun Pile, Transverse Reinforcement

## 1. Introduction

The strength of a structural member was designed

according to the internal forces including bending moments that occurred due to the applied load. For reinforced concrete columns, the design involves the interaction of axial and bending moment (P-M) diagrams. Based on the P-M diagram, the capacity of the cross-section can be obtained from the results of the cross-sectional strain distribution due to axial forces and bending moments analysis. Therefore, a hollow cross-section requires a different calculation for the concrete compression area than conventional cross-sections, and Figure 1 shows a more thorough look at the computation of stress block modeling.

The presence of confinement affected the actual stress-strain curve, particularly the increase in compressive stress of concrete at the peak and post-peak until its ultimate strain [1]. Confining actions on concrete can be achieved by various types of efforts, namely external/internal confinement, spiral/stirrups, fiber/wire mesh, etc. [2,3]. The ultimate strain of confined concrete is the most important parameter to be defined for the ductility in concrete, which was influenced by confinement provided by transverse steel [4]. By taking into account the influence of confinement, the ultimate strain of concrete increases, resulting in a more ductile manner of concrete or structural members such as beams, columns, and piles [3,4]. The Hognestad model [5] from 1951 was used in conjunction with the unconfined formulation to compute the stress-strain curve of concrete without any constraints. This model was frequently utilized since its output was remarkably accurate. The Mander et al. [6], El-Dash and Ahmad [7], and Kusuma and Tavio [8] models were

utilized as the common confinement models.

The application of spun piles is common in Indonesia, but as is known, hollow sections have poor ductility compared to solid sections. Providing concrete confinement can improve the ductility of reinforced concrete sections by considering the impact of confinement and the increase of the ultimate strain to the improvement of the ductility of the structure [9-14]. By specifying the internal forces, it will be possible to ensure that there are no problems that appear during construction because the pile will encounter a bending force caused by the pile load itself throughout the lifting process [15,16]. The condition of balanced strain (strain compatibility) was achieved when a tensile reinforcement strain of  $\epsilon_y$  was combined with the maximum strain  $\epsilon_c$  at the maximum compressive fiber of concrete [17]. In the analysis of the cross-section, 25% of the prestress component represents all prestress loss components.

## 2. Objectives

Among the study's research objectives are the following:

- 1) Monitor the pile's bending moment capacity when the pre-stressing force is increased.
- 2) Check the impact of stirrup spacing on the nominal capacity of constrained concrete sections.
- 3) Determine whether the breadth of the confinement affects the concrete section's constrained nominal capacity.
- 4) Determine the form of the concrete-confined axial-moment interaction diagram.

- 5) Determine how the restriction on the spun pile affects curvature ductility.

## 3. Methods

### 3.1. MATLAB Program

Spun Pile Analysis (SPA ver. 1.0) is the latest program used to draw interaction diagrams and moment-curvature of a spun pile cross-section according to the input given based on the ACI 318-19 method [18]. The data required as input to the program are material properties, dimensions of the spun pile, reinforcement data, and the initial prestress force. Next, determine the restraint method used and proceed to the calculation of stress block, pre-stress reinforcement spacing, and internal force due to pre-stress reinforcement. The next calculation is neutral line iteration to obtain the stress of each pre-stressing steel used to calculate axial and moment. Graphical plotting of the interaction and moment-curvature diagrams of the spun pile cross-section are concluded. The use of the SPA ver. 1.0 program can replace the time-consuming trial and error calculation of manual cross-section neutral lines.

The sub-menu area is used to input data that will eventually serve as computation data in the MATLAB application script. Based on the input data value, the output of the SPA ver. 1.0 is the nominal interaction diagram and the notional axial moment capacity (and its combinations) of the cross-section. The results of the diagram are used to determine the axial capacity, moment, and value of the ductility curve of the pile section.

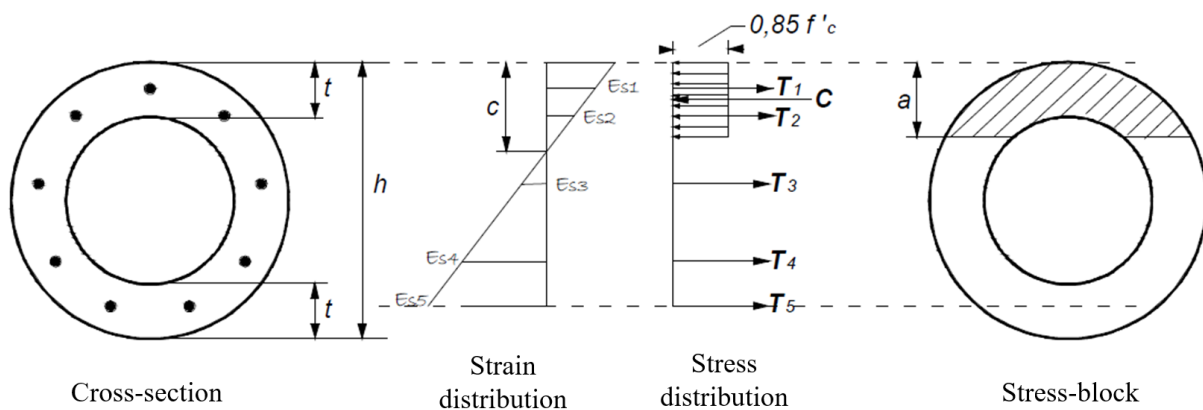


Figure 1. Stress-block modeling of hollow piles.

### 3.2. Program Outcome Validation

Only a few studies exist that discuss the moment-curvature of spun piles experimentally. Budek and Priestley [19] investigated the flexibility of hollow prestressed piles and discovered one of them. To characterize plastic hinge development, four half-scale precast prestressed pile models were tested under flexural conditions. The test apparatus simulated the pile's in-situ subgrade moment pattern as well as the external restraint of the soil around the pile shaft. The experimental results (PS12) were compared to those of the SPA ver. 1.0 program, as shown in Figure 2. The graph shows significant differences due to the different restraint models used, but the results are all close to each other.

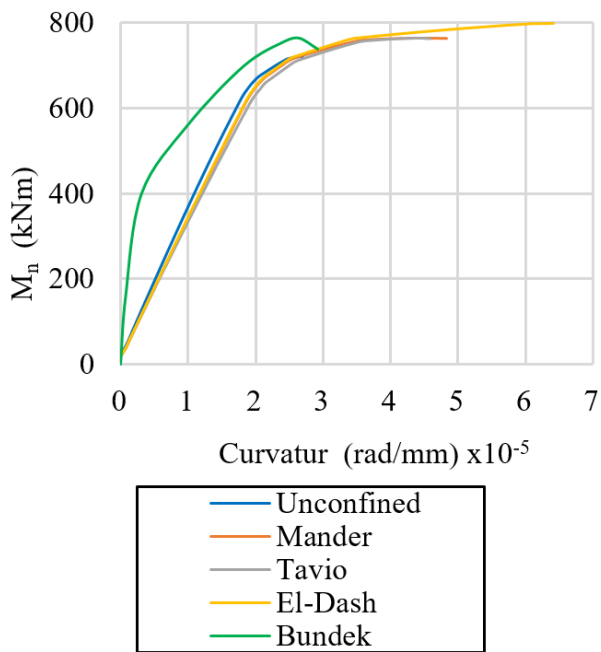


Figure 2. Momen-curvature comparison.

Table 1a. Manual Calculation Axial Value vs SPA ver. 1.0

Neutral Axis (c)	Pn (kN)		
	Manual	Program	Different (%)
-	6167.13	7191.40	16.61
798.34	6480.84	6480.80	0.00
617.89	4684.12	4684.10	0.00
302.78	2493.81	2493.80	0.00
127.46	456.50	456.50	0.00

The results of axial and moment comparisons between manual calculations and the SPA ver. 1.0 program are shown in Tables 1a and 1b. Table 1a shows a 16.61% difference in the P<sub>n</sub> value because the program iteration is only limited to the height of the cross-section. A

straight-line equation is used to continue the curve, giving a manual P<sub>n</sub> calculation number that is different from the computer findings. Other results show a 0% difference, indicating that the numerical method approach used by the computer is relatively more thorough and accurate.

Table 1b. Manual Calculation Moment Value vs SPA ver. 1.0

Neutral Axis (c)	Mn (kNm)		
	Manual	Program	Different (%)
-	0.00	0.00	0.00
798.34	183.93	183.93	0.00
617.89	516.81	516.81	0.00
302.78	567.98	567.98	0.00
127.46	373.25	373.25	0.00

### 3.3. Hollow Pile Modeling

The created program receives the data from Table 2 as input, and the output results take the shape of a graph with pile interactions. For the accuracy of the developed program, a control check for the outcomes of the running program is required, specifically for the condition of the cross-section's maximum axial capacity, the condition of the maximum moment, and various axial moment combinations points. The spun pile requirements utilized as a research instrument in analysis modeling are as follows:

- $f'_c = 60$  MPa (Concrete)
- $f_{up} = 1860$  MPa (PC Wire)
- $f_{yp} = 1670$  MPa (PC Wire)
- $f_{yh} = 647$  MPa (Spiral)
- $h = 600$  mm (Spun Pile Diameter)
- $t = 100$  mm (Spun Pile Thickness)
- $n_p = 8$  (Number of PC Wire)
- $d_p = 12.7$  mm (PC Wire Diameter)

Table 2. Model data to be simulated

Specimen code	Effective Stress, $f_{eff}$ (MPa)	Spacing of Spirals, $s_h$ (mm)	Spiral Diameter, $d_s$ (mm)
M1a	976.500	100	8
M2a	697.500	100	8
M3a	348.750	100	8
M1b	976.500	100	8
M2b	976.500	150	8
M3b	976.500	200	8
M1c	976.500	100	4
M2c	976.500	100	8
M3c	976.500	100	10

## 4. Result and Discussions

After the pre-stressed pile interaction diagram program

has been obtained and the output results have been checked, the next step is to analyze the effect of confinement on the pile capacity, which is known through the nominal ability value of the axial cross-section and the moment with the following cases.

**4.1. Influence of Prestress Force on Cross-Sectional Capacity**

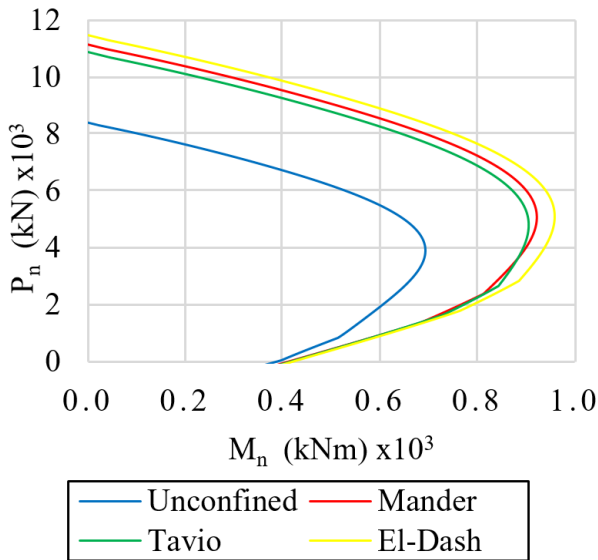


Figure 3. Increase in nominal capacity of pre-stressed piles model M1a.

Pre-stressed force is internal compressive stress applied to concrete that reduces the potential tensile stress in concrete due to working load (ACI 318-19). At the jacking stage, a tendon-pulling tool and pivots are used to provide the initial prestressing force. When the concrete is at the set age, the tendon is disconnected to transfer the tendon's tensile forces to the concrete (pre-tensioned system).

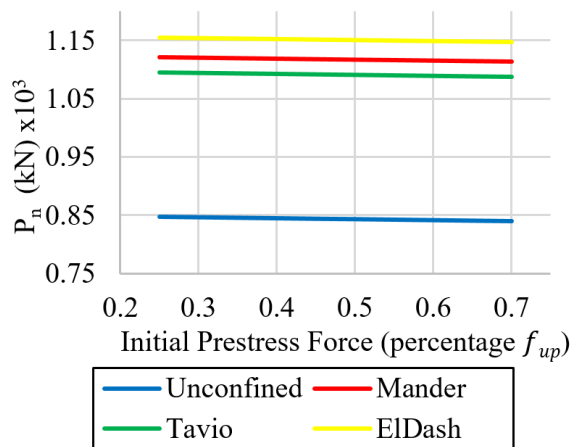


Figure 4. Comparison of nominal capacity due to pre-stress force.

Figure 4 depicts a more pronounced effect of prestress force on maximum axial capacity. As the applied prestress force increases, the axial value decreases hardly. For the unconfined cross-section, the decrease is 0.105% for each 5% increase in prestress force. The difference in value between specimens occurs because the  $f_{eff}$  value is used to calculate the  $f_{si}$  value, which is then used to calculate the initial strain of the prestressed reinforcement when exposed to prestressing forces. When computing the internal forces, the strain value of each reinforcement will be affected, increasing the maximum  $P_n$  value.

In contrast to the cross-section with confinement, the percentage of decrement per 5% increase in prestress force is 0.078%, which is lower than the percentage of decrease in the cross-section without confinement due to the constant decrease in value of 0.9 kN for all methods. The percentage value decrease in the cross-section with confinement is lower than the cross-section without confinement due to the difference in axial values in the cross-sections without and with confinement caused by the lateral force.

**4.2. Influence of Spiral Restraint Density on Cross-Sectional Capacity**

Table 1 summarizes the changes in spiral spacing to test the effectiveness of spiral spacing in increasing the nominal capacity of reinforced concrete cross-sections. The results shown in Figure 5 are the interaction diagram of specimen M2b. When the spiral spacing value is 150, the cross-section with restraint shows a diagram that almost coincides. Figures 6 and 7 have been created to summarize the results of the maximum values of each axial and moment values obtained from the output of the SPA ver 1.0 program.

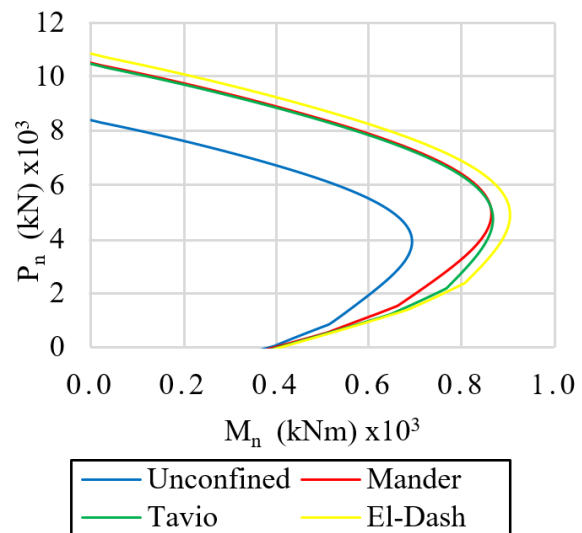


Figure 5. Comparison of the P-M interaction diagram of the M2b case.

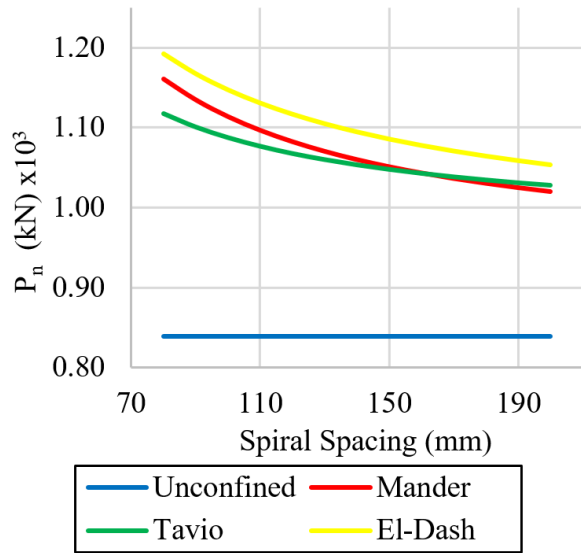


Figure 6. Maximum axial value due to spiral spacing comparison.

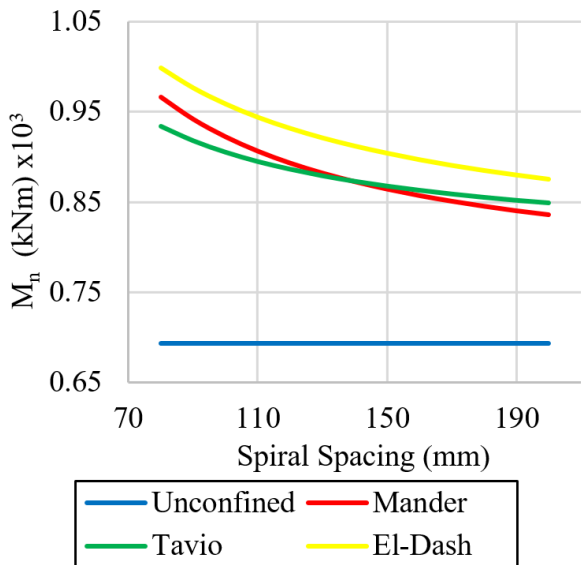


Figure 7. Maximum moment value due to spiral spacing comparison.

In specimen B, the cross-section without confinement did not affect the maximum axial or maximum moment due to the spiral spacing. On the contrary, different values appear in the cross-section with confinement. Every 10 mm increase in spiral spacing results in a 0.929% decrease in maximum axial value. The maximum moment value decreases in value by 1.025% for every 10 mm increase in spiral spacing. The axial and moment capacity values of the cross-section with confinement decreased as the spiral spacing expanded. That's also due to the spiral spacing used in the stress-strain curve calculation of each method. With an expansion in spiral spacing, the compressive strength of concrete ( $f_{cc}$ ) decreased.

### 4.3. Influence of Spiral Reinforcement Area on Cross-Sectional Capacity

To handle the high pressures at anchorage and to give strength to the thinner sections of the pile sections, stronger concrete is needed. The strength of the section will rise as a result of lateral stresses brought on by confinement. To ascertain its impact on the nominal capacity of the confined concrete section, the area of confinement reinforcement is increased and examined.

Figure 8 depicts the interaction diagram resulting from specimen M1c. From the figure, axial and moment capacity values are smaller than the previous specimens due to the use of a spiral diameter of 4 mm. It also showed a fracture in the diagram for all models caused by the first yield of the tendon reinforcement.

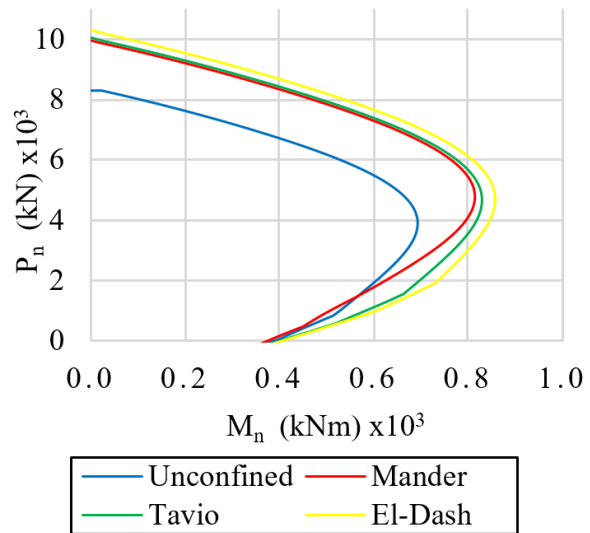


Figure 8. Interaction diagram of the M1c model pre-stressed pile.

Figures 9 and 10 summarize the effect of the confinement reinforcement area. The axial and moment values for the cross-section without confinement remain unchanged from the previous case, at 839.4 kN and 693.06 kN-m, respectively. Significant changes can be shown in the confined cross-section, with the average axial capacity increasing by 1.391% for each 5 mm increase in diameter dimension. A similar increase in value occurs in moment capacity, where each 5 mm increase in diameter increases average axial capacity by 1.513%. These findings suggest that a bigger spiral diameter will have an impact on the confined concrete section's addition of axial capacity as well as the moment and that the confined concrete pile has a higher axial-moment capacity than the unconfined concrete pile. This is due to the lateral force acting on the confined concrete, which increases both the compressive strength ( $f_{cc}$ ) and the area of the constricting reinforcement.

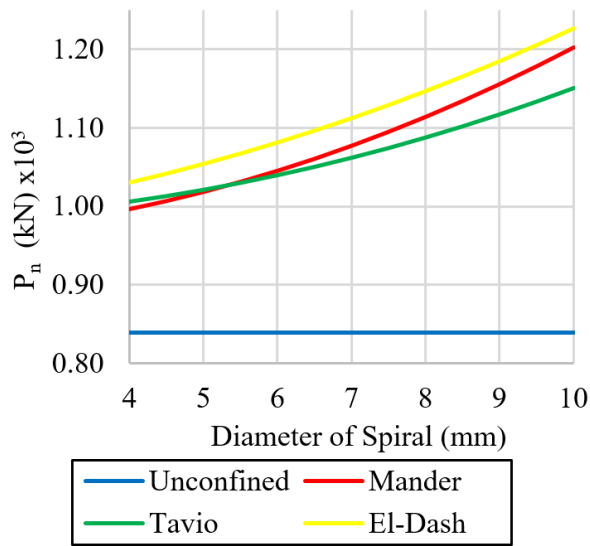


Figure 9. Maximum axial value due to spiral reinforcement area comparison.

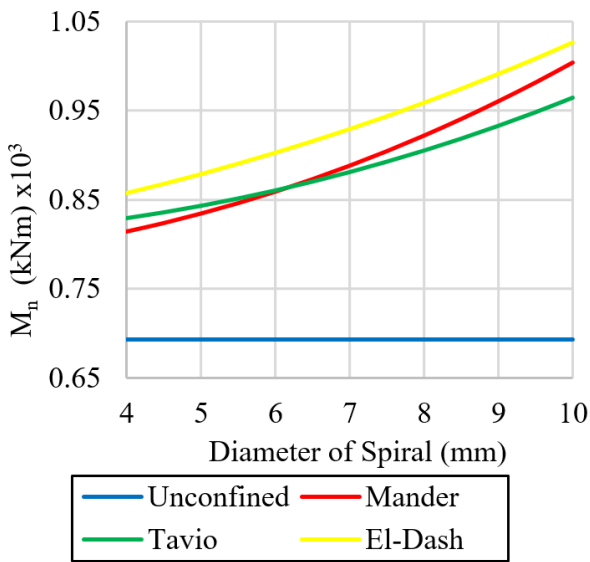


Figure 10. Maximum moment value due to spiral reinforcement area comparison.

4.4. Influence of Confinement on Curvature Ductility

Ductility is required in reinforced concrete elements to create structures that are relatively strong and economical. The reinforcing of the confinement has an impact on the ductility calculation. We have covered the impact of spiral spacing and the impact of increasing the amount of confinement reinforcement in the previous two models.

The moment-curvature diagram, shown in Figures 11 and 12, is another output of the SPA ver. 1.0 program. Figure 11 depicts the effect of spiral spacing, while Figure 12 depicts the effect of reinforcement area confinement. Each figure demonstrated that the curvature value of the

cross-section with confinement is much greater than the curvature value of the cross-section without confinement. This affects the ductility values shown in Figures 13 and 14.

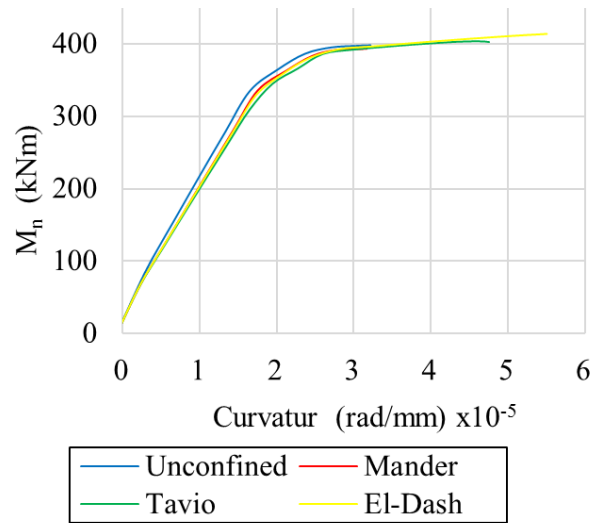


Figure 11. Moment-curvature diagram of the M3b model pre-stressed pile.

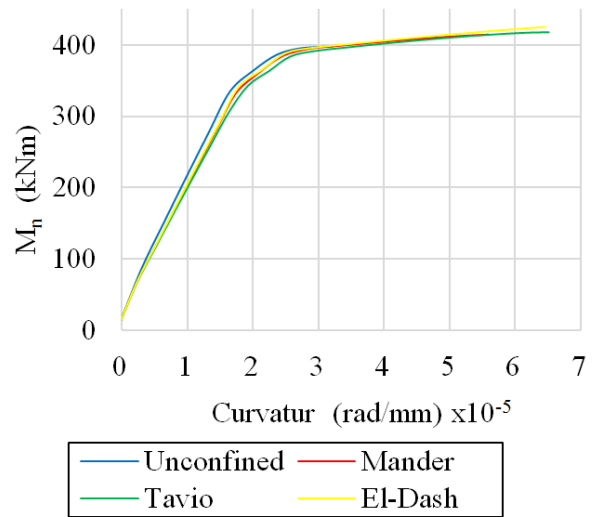


Figure 12. Moment-curvature diagram of the M2c model pre-stressed pile.

Figures 13 and 14 show that the result of unconfined ductility has a constant value of 1.36 when both spiral spacing and spiral reinforcement areas are considered. However, the value of confined concrete produced by each method differs. The average value of curvature ductility decreased by 4.338% when the spiral spacing was increased by 10 mm. While raising the diameter for each 5 mm increased the curvature ductility by 6.947%. This is because the final strain formulation of each method produces different results. Furthermore, the stress-strain curve equation from each method, which takes a different approach, will influence the results. The stress-strain curve equation has an impact on the value.

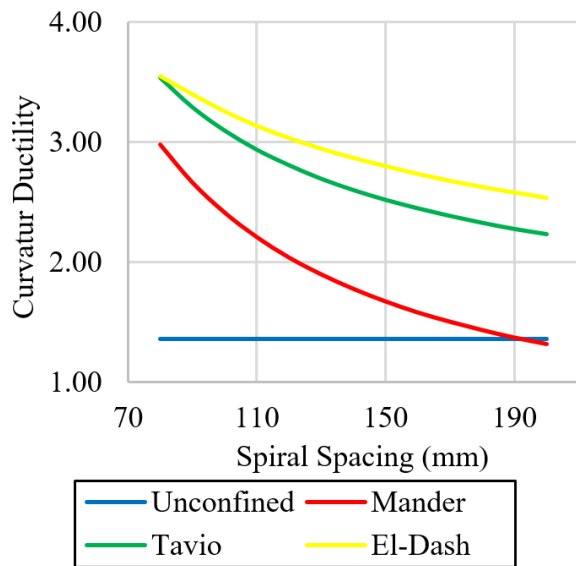


Figure 13. Comparison of ductility value due to spiral spacing.

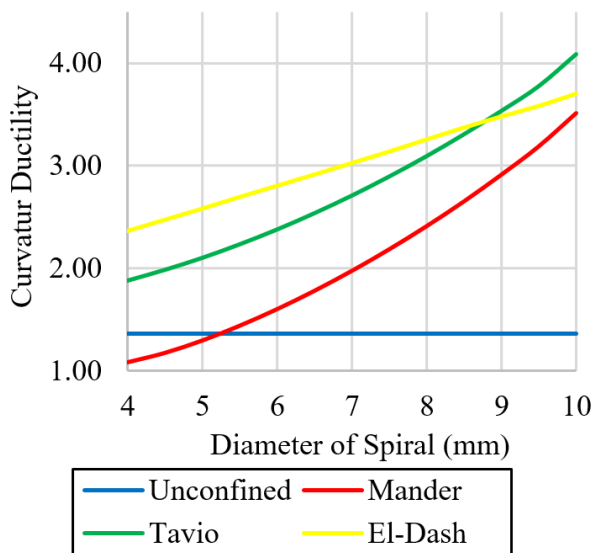


Figure 14. Comparison of ductility values due to spiral reinforcement area.

## 5. Conclusions

The following conclusions can be drawn from the results of the spun pile model:

- 1) Every 5% increase in prestressing force reduces axial capacity by 0.105% for cross sections without confinement and 0.078% for cross sections with confinement.
- 2) The axial capacity and moment in the cross section will decrease with confinement due to the addition of spiral spacing by 0.929% and 1.025%, respectively.
- 3) Changing the spiral diameter dimension every 5 mm increases the axial and moment capacity values by an average of 1.391% and 1.513%.

- 4) Curvature ductility decreases by 4.338% as spiral spacing increases by 10 mm. In contrast, the curvature ductility value increases by 6.947% for every 5 mm increase in diameter dimension.

## Acknowledgements

The authors also gratefully acknowledge the financial support received from the Institut Teknologi Sepuluh Nopember for this work, under the project scheme of the Publication Writing and IPR Incentive Program (PPHKI) 2023.

## REFERENCES

- [1] Tavio, and Kusuma B., Stress-strain model for high-strength concrete confined by welded wire fabric, *Journal of Materials in Civil Engineering*, ASCE, vol. 21, no. 1, 40-45, 2009.
- [2] Tavio, Anggraini R., Raka I G. P., and Agustiar, Tensile strength/yield strength (TS/YS) ratios of high-strength steel (HSS) reinforcing bars, *AIP Conference Proceedings*, vol. 1964, no. 020036, 1-8, 2018.
- [3] Pudjisyadi P., and Tavio, Axial compressive behavior of square concrete columns externally collared by light structural steel angle sections, *International Journal of Applied Engineering Research*, vol. 11, no. 7, 4655-4666, 2016.
- [4] Agustiar, Raka I G. P., and Anggraini R., Behavior of concrete columns reinforced and confined by high-strength steel bars, *International Journal of Civil Engineering and Technology*, vol. 9, no. 7, 1249-1257, 2018.
- [5] Hognestad, A study of combined bending and axial load in reinforced concrete members, *University of Illinois*, vol. 49, no. 399, 1-6, 1951.
- [6] Mander J. B., Priestley M. J. N., and Park R., Theoretical stress-strain model for confined concrete, *J. Struct. Eng.*, vol. 114, no. 8, 1804-1826, 1988.
- [7] El-Dash K. M. and El-Mahdy O. O., Modeling the stress-strain behavior of confined concrete columns, *Am. Concr. Institute, ACI Spec. Publ.*, vol. SP-238, no. February 2015, 177-192, 2006.
- [8] Tavio and Kusuma B., Unified stress-strain model for confined columns of any concrete and steel strengths, in *International Conference on Earthquake Engineering and Disaster Mitigation*, no. 1980, 510-517, 2008
- [9] El-Dash K. M. and Ahmad S. H., A model for stress-strain relationship of spirally confined normal and high-strength concrete columns, *Mag. Concr. Res.*, vol. 47, no. 171, 177-184, 1995.
- [10] Bouafia Y., Iddir A., Kachi M. S., and Dumontet H., Stress-strain relationship for the confined concrete, 11<sup>th</sup> World Congr. Comput. Mech. WCCM 2014, 5th Eur. Conf. Comput. Mech. ECCM 2014 6th Eur. Conf. Comput. Fluid

- Dyn. ECFD 2014, no. Wccm Xi, 1593–1603, 2014.
- [11] Cusson D. and Paultre P., High strength concrete columns confined by rectangular ties, *J. Struct. Eng.*, vol. 120, no. 3, 783–804, 1994.
- [12] Popovics S., A numerical approach to the complete stress-strain curves for concrete, *Cem. Concr. Res.*, vol. 3, no. 5, 583–59, 1973.
- [13] Heerema P. S., Cylindrical hollow prestressed concrete piles, *PCI Journal*, vol. 5, no. 4, 41–47, 1960.
- [14] Sheppard D. A., Seismic design of prestressed concrete piling, *PCI Journal*, vol. 28, no. 2, 20–49, 1983.
- [15] Muthukkumaran K., Keerthi Raaj S., and Vinoth Kumar M., Assessment of pile failures due to excessive settlement during pile load test, 15th Asian Reg. Conf. Soil Mech. Geotech. Eng. ARC 2015 New Innov. Sustain., Nov., 2520–2524, 2015.
- [16] Lee C. H., Kang T. H. K., Kim S. Y., and Kang K., Strain compatibility method for the design of short rectangular concrete-filled tube columns under eccentric axial loads, *Constr. Build. Mater.*, vol. 121, 143–153, 2016.
- [17] Abdel-Jaber H. and Glisic B., Monitoring of prestressing forces in prestressed concrete structures-An overview, *Struct. Control Heal. Monit.*, vol. 26, no. 8, 1–27, 2019.
- [18] ACI Committee 318, Building code requirements for structural concrete and commentary (ACI 318-19), American Concrete Institute, Farmington Hills, Michigan USA, 624, 2019.
- [19] Budek A. M. and Priestley M. J. N., Experimental analysis of flexural hinging in hollow marine prestressed pile shafts, *Coast. Eng. J.*, vol. 47, no. 1, pp. 1–20, 2005.